J|A|C|S
ARTICLES
Published on Web 10/14/2004

Developing Photoactive Affinity Probes for Proteomic Profiling: Hydroxamate-based Probes for Metalloproteases

Elaine W. S. Chan,[†] Souvik Chattopadhaya,[‡] Resmi C. Panicker,[†] Xuan Huang,[†] and Shao Q. Yao*[,†,‡]

Contribution from the Department of Chemistry and Department of Biological Sciences, National University of Singapore, 3 Science Drive 3, Singapore 117543, Republic of Singapore

Received May 20, 2004; E-mail: chmyaosq@nus.edu.sg

Abstract: The denaturing aspect of current activity-based protein profiling strategies limits the classes of chemical probes to those which irreversibly and covalently modify their targeting enzymes. Herein, we present a complimentary, affinity-based labeling approach to profile enzymes which do not possess covalently bound substrate intermediates. Using a variety of enzymes belonging to the class of metalloproteases, the feasibility of the approach was successfully demonstrated in several proof-of-concept experiments. The design template of affinity-based probes targeting metalloproteases consists of a peptidyl hydroxamate zinc-binding group (ZBG), a fluorescent reporter tag, and a photolabile diazirine group. Photolysis of the photolabile unit in the probe effectively generates a covalent, irreversible linkage between the probe and the target enzyme, rendering the enzyme distinguishable from unlabeled proteins upon separation on a SDS-PAGE gel. A variety of labeling studies were carried out to confirm that the affinity-based approach selectively labeled metalloproteases in the presence of a large excess of other proteins and that the success of the labeling reaction depends intimately upon the catalytic activity of the enzyme. Addition of competitive inhibitors proportionally diminished the extent of enzyme labeling, making the approach useful for potential in situ screening of metalloprotease inhibitors. Using different probes with varying P_1 amino acids, we were able to generate unique "fingerprint" profiles of enzymes which may be used to determine their substrate specificities. Finally, by testing against a panel of yeast metalloproteases, we demonstrated that the affinity-based approach may be used for the large-scale profiling of metalloproteases in future proteomic experiments.

Introduction

Great advances in genome research have been made in recent years, the completion of the human genome project in 2001 being a major milestone.[1] However, proteins, rather than genes, are ultimately responsible for most biological processes occurring inside the cell and therefore are tightly regulated by a variety of post-DNA/RNA processes including control of expression levels, compartmentalization to different subcellular organelles, post-transcriptional and post-translational modifications.[2] A conservative estimate of the number of structurally and functionally diverse proteins expressed in the human genome places the figure at a minimum of 100 000, far exceeding the number of estimated human genes (30 000−40 000).[1] Thus the major aim of proteomics has been to identify, characterize, and assign biological functions for all proteins expressed by the genome.[3] To accomplish this Herculean effort, major research activities in the post-genomic era focus on the development of high-throughput methods which can be utilized for the large-scale studies of proteins, including their expression levels, cellular functions, localization, and interaction networks.[4−6]

Traditionally, two-dimensional gel electrophoresis (2D-GE) has been the work horse for large-scale protein expression analysis. More recently, 2D-GE, when combined with advanced mass spectrometric techniques, has become the state-of-the-art method for major proteomic research, primarily due to its ability to analyze up to a few thousand protein spots in a single experiment.[4a] By simultaneous analysis of the relative abundance of endogenous proteins present in a biological sample, 2D-GE allows for the identification of important protein biomarkers associated with changes in the cellular/physiological state of the sample. Most techniques based on 2D-GE, however, suffer from a number of serious technical problems: low detection

[†] Department of Chemistry.
[‡] Department of Biological Sciences.

(1) Venter, J. C. et al. *Science* **2001**, *291*, 1304−1351.
(2) Tyers, M.; Mann, M. *Nature* **2003**, *422*, 193−197.
(3) Fields, S. *Science* **2001**, *291*, 1221−1224.
(4) (a) Aebersold, R.; Mann, M. *Nature* **2003**, *422*, 198−207. (b) Huang, X.; Tan, E. L. P.; Chen, G. Y. J.; Yao, S. Q. *Appl. Genomics Proteomics* **2003**, *2*, 225−238. (c) Patton, W. F. *Electrophoresis* **2000**, *21*, 1123−1144. (d) Gygi, S. P.; Rist, B.; Gerber, S. A.; Turecek, F.; Gelb, M. H.; Aebersold, R. *Nat. Biotechnol.* **1999**, *17*, 994−999. (e) Monribot-Espagne, C.; Boucherie, H. *Proteomics* **2002**, *2*, 229−240. (f) Unlu, M.; Morgan, M. E.; Minden, J. S. *Electrophoresis* **1997**, *18*, 2071−2077.
(5) For reviews, see: (a) MacBeath, G. *Nat. Genet.* **2002**, *32*, 526−532. (b) Chen, G. Y. J.; Uttamchandani, M.; Lue, R. Y. P.; Lesaicherre, M. L.; Yao, S. Q. *Curr. Top. Med. Chem.* **2003**, *3*, 705−724. (c) Braun, P.; LaBaer, J. *Drug Discuss. Today* **2004**, *9*, s1. (d) Schweitzer, B.; Predki, P.; Snyder, M. *Proteomics* **2003**, *3*, 2190−2199.
(6) (a) Huh, W. K.; Falvo, J. V.; Gerke, L. C.; Carroll, A. S.; Howson, R. W.; Weissman, J. S.; O'Shea, E. K. *Nature* **2003**, *425*, 686−691. (b) Ghaemmaghami, S.; Huh, W.; Bower, K.; Howson, R. W.; Belle, A.; Dephoure, N.; O'Shea, E. K.; Weissman, J. S. *Nature* **2003**, *425*, 737−741. (c) Ho, Y. et al. *Nature* **2002**, *415*, 180−183. (d) Gavin, A. et al. *Nature* **2002**, *415*, 141. (e) Uetz, P. et al. *Nature* **2000**, *403*, 623−627.

sensitivity, limited dynamic range, and low reproducibility. Furthermore, when compared with other existing protein analysis techniques, perhaps the major shortcoming of 2D-GE techniques is that it gives rise to a restricted amount information about proteins such as their identity and relative abundance. In most cases, no information about the biological function of a protein can be delineated from the 2D-GE experiment.[4b]

Over the years, different variations of 2D-GE have been developed in order to address some of these issues.[4c−f] For example, a number of fluorescence-based protein detection methods were developed, which allow highly sensitive detection of low-abundant proteins on a 2-D gel over a broad linear dynamic range.[4c] Various strategies, including ICAT, isotope-based metabolic labeling and DIGE, have been developed, allowing protein samples from different cellular states to be simultaneously separated and analyzed, thus ensuring quantitative comparison of the protein expression levels.[4d−f] Emerging technologies such as microarray-based technologies have shown great promise in being the ultimate high-throughput tool for future proteomic research.[5] With the protein array technology, for example, it has been shown that it is possible to immobilize the entire protein complement of yeast (e.g. ~6000 yeast ORFs) onto a 2.5 × 7.5 cm^2 glass surface, where different biological functions of all yeast proteins could be studied simultaneously.[5d] To bridge the gap between technologies such as the protein microarray, which primarily analyze purified proteins, and 2D-GE based techniques, which study endogenous proteins by their expression, and combine the high-throughput feature of 2D-GE with the ability of function-based protein studies, a chemical proteomics approach was recently developed, which enables the activity-based profiling of enzymes on the basis of their activity, rather than their levels of abundance.[7] The general strategy in activity-based profiling typically involves a small molecule-based, active site-directed probe which targets a specific class of enzymes based on their enzymatic activity. The design template for activity-based probes essentially comprises a reactive unit, a linker unit, and a reporter unit, in which the reactive unit is made of a mechanism-based inhibitor of a class of enzymes. By reacting with the targeting enzymes in an activity-dependent manner, the reactive unit serves as a "warhead" to covalently modify the enzyme, thus rendering the resulting probe−enzyme adducts easily distinguishable from other unmodified proteins. The reporter unit in the probe is either a fluorescence tag for sensitive and quantitative detection of labeled enzymes or an affinity tag (e.g., biotin) which facilitates further protein enrichment/purification/identification. A number of activity-based probes have thus far been reported, some of which have been successfully used for proteomic profiling of different enzymatic classes in complex proteomes.[7] For example, fluorophosphonate/fluorophosphate derivatives have been developed to selectively profile serine hydrolases, including serine proteases.[8a,b] For cysteine proteases, different classes of chemical probes have been reported, including probes containing α-halo or (acyloxy) methyl ketone substituents, epoxy- and vinyl sulfone-derivatized peptides.[8c−g] Other known activity-based probes include sulfonate ester-containing probes that target a few different classes of enzymes,[8h] as well as probes conjugated to *p*-hydroxymandelic acid which specifically label protein phosphatases.[8i,j] However, to date, there has been no report on activity-based probes capable of profiling aspartic proteases or metalloproteases, which constitute the other two major classes of proteases. This is due to the lack of known mechanism-based inhibitors that form covalent adducts with these enzymes, a prerequisite of most existing activity-based chemical profiling approaches.

This paper describes a complimentary strategy for proteomic profiling of enzymes without the need of mechanism-based suicide inhibitors. Our strategy utilizes chemical probes that are made up of reversible inhibitors of enzymes (Figure 1). Each probe has an affinity binding unit, a specificity unit, and a photolabile group. The affinity unit comprises a known reversible inhibitor that binds tightly in a noncovalent manner to the active site of the target enzyme (or a specific class of target enzymes). A wealth of information on noncovalent inhibitors of enzymes is known, thus making our approach applicable to target most classes of enzymes. The specificity unit, on the other hand, could be a specific peptide sequence serving as the recognition group of the target enzyme or a simple linker which confers minimum substrate specificity toward most enzymes in the same class. Because the enzyme−probe interaction is solely based on affinity, an additional moiety, the photolabile group, is required in our strategy to effect a permanent attachment of the probe to the enzyme. The incorporation of a fluorescent tag eventually results in a trifunctional affinity-based probe for potential large-scale protein profiling experiments (Figure 1a). Photoaffinity labels, such as those containing diazirine or benzophenone, have been used to covalently modify molecules in a variety of biological experiments.[9] These photoactive labels operate by generating reactive intermediates such as carbenes, nitrenes, and ketyl biradicals and inserting them into the target molecule to form a permanent cross-linkage.[10] The selected wavelength for UV irradiation is usually greater than 300 nm, thus preventing potential photochemically induced damage to the enzyme. Overall, our affinity-based approach takes advantage of the reversible inhibitor of an enzyme which functions as the "Trojan Horse" (Figure 1b): it first ferries the photolabeled affinity probe to the enzyme active site. Upon UV irradiation, the photolabile group in the probe irreversibly modifies the enzyme and forms a covalent enzyme−probe adduct, which renders the enzyme distinguishable from unlabeled proteins on a denaturing SDS gel. Recently, this concept was independently reported by Hagenstein et al.,[11] whereby benzophenone-tagged isoquinolinesulfonamides were utilized

(7) For recent reviews, see: (a) Cravatt, B. F.; Sorensen, E. J. *Curr. Opin. Chem. Biol*. **2000**, *4*, 663−668. (b) Jeffery, D. A.; Bogyo, M. *Curr. Opin. Biotechnol*. **2003**, *14*, 87−95.

(8) (a) Liu, Y. S.; Patricelli, M. P.; Cravatt, B. F. *Proc. Natl. Acad. Sci. U.S.A.* **1999**, *96*, 14694−14699. (b) Kidd, D.; Liu, Y. S.; Cravatt, B. F. *Biochemistry* **2001**, *40*, 4005−4015. (c) Faleiro, L.; Kobayashi, R.; Fearnhead, H.; Lazebnik, Y. *EMBO J.* **1997**, *16*, 2271−2281. (d) Liau, M. L.; Panicker, R. C.; Yao, S. Q. *Tetrahedron Lett.* **2003**, *44*, 1043−1046. (e) Greenbaum, D.; Medzihradszky, K. F.; Burlingame, A.; Bogyo, M. *Chem. Biol*. **2000**, *7*, 569−581. (f) Nizif, T.; Bogyo, M. *Proc. Natl. Acad. Sci. U.S.A.* **2001**, *98*, 2967−2972. (g) Wang, G.; Uttamchandani, M.; Chen, G. Y. J.; Yao, S. Q. *Org. Lett.* **2003**, *5*, 737−740. (h) Adam, G. C.; Sorensen, E. J.; Cravatt, B. F. *Nat. Biotechnol*. **2002**, *20*, 805−809. (i) Lo, L. C.; Pang, T. L.; Kuo, C. H.; Chiang, Y. L.; Wang, H. Y.; Lin, J. J. *J. Proteome Res.* **2002**, *1*, 35−40. (j) Zhu, Q.; Huang, X.; Chen, G. Y. J.; Yao, S. Q. *Tetrahedron Lett.* **2003**, *44*, 2669−2672.

(9) Lopez-Otin, C.; Overall, C. M. *Nature Rev. Mol. Cell Biol*. **2002**, *3*, 509−519.

(10) (a) Dorman, G. *Top. Curr. Chem*. **2001**, *211*, 169−225. (b) Dorman, G.; Prestwich, G. D. *Trends Biotechnol*. **2000**, *18*, 64−67. (c) Kotzyba-Hibert, F.; Kapfer, I.; Goeldner, M. *Angew. Chem., Int. Ed. Engl*. **1995**, *34*, 1296−1312. (d) Fleming, S. A. *Tetrahedron* **1995**, *51*, 12479−12520. (e) Brunner, J. *Annu. Rev. Biochem*. **1993**, *62*, 483514. (f) Dorman, G.; Prestwich, G. D. *Biochemistry* **1994**, *33*, 5661−5673.

(11) Hagenstein, M. C.; Mussgnug, J. H.; Lotte, K.; Plessow, R.; Brockhinke, A.; Kruse, O.; Sewald, N. *Angew. Chem., Int. Ed.* **2003**, *42*, 5635−5638.

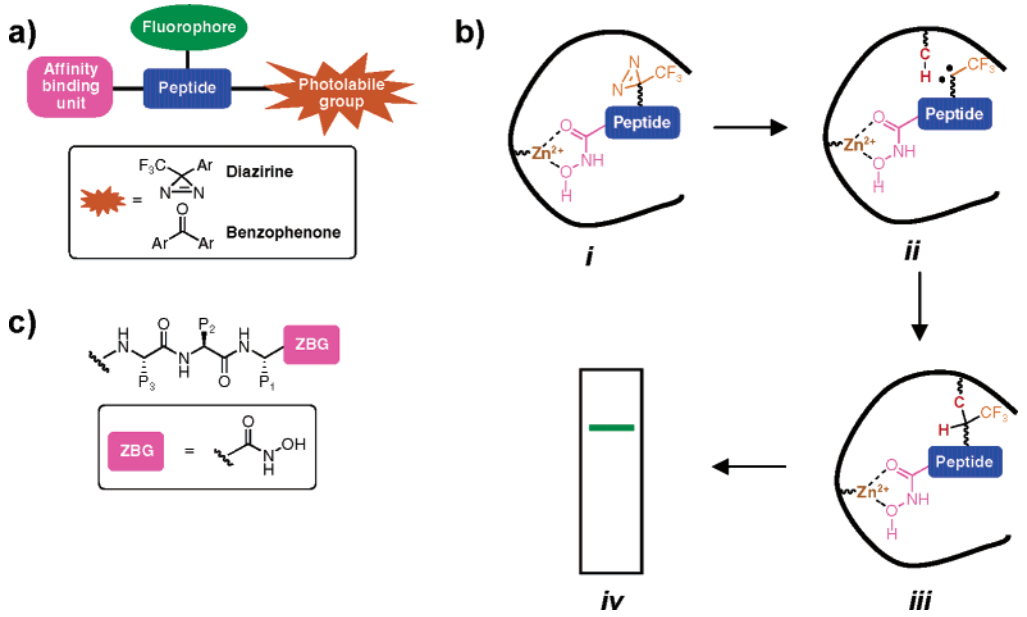

Figure 1. (a) Schematic representation of probes for affinity-based proteomic profiling; (b) schematic representation of affinity-based profiling of metalloproteases: (i) hydroxamate zinc-binding group chelates to zinc; (ii) irradiation of the photolabile group by UV light causes the diazirine group to fragment into a carbene; (iii) the carbene inserts covalently into any nearby C−H bonds in the vicinity of the active site; (iv) upon denaturation prior to SDS-PAGE analysis, the affinity probe is still bound to the enzyme even though the hydroxamate has been released by the active site; (c) left-hand side (LHS) peptidylmetalloprotease inhibitors, ZBG = zinc-binding group.

in the functional labeling of kinases. In this report, we demonstrate the feasibility of this affinity-based strategy for the large-scale proteomic profiling of metalloproteases using hydroxamate-containing photoaffinity probes (Figure 1c).[12]

Materials and Methods

General Information. For general material information and synthetic procedures of **1**−**3**, see Supporting Information.

General Procedure for Synthesis of GGX-NHO-Resin (4). Resin **3** was prepared from Fmoc (9-fluorenylmethyloxycarbonyl)-NHOH and 2-chlorotrityl chloride resin as previously described.[13] Subsequently, 100 mg of resin **3** was placed into a 5 mL reaction vessel provided with the Quest 210 organic synthesizer. To attach the first amino acid to the resin, the coupling reaction was carried out for 24 h. The resin was preswelled in DMF for 1 h. In a separate reaction vessel, Fmoc-amino acid (4 equiv), TBTU (2-(1-*H*-benzotriazol-1-yl)-1,1,3,3-tetramethyluronium tetraborofluorate) (4 equiv), and HOBt (4 equiv) were dissolved in a minimum amount of DMF. DIEA (*N*,*N*′-diisopropylethylamine) (8 equiv) was then added, and the reaction mixture was shaken for 10 min. The solution was subsequently added to the resin. The resulting reaction mixture was then agitated on the synthesizer for 24 h, after which the reagents were drained. The resin was washed (with DMF, DCM (dichloromethane), and MeOH sequentially) and dried in vacuo overnight. Quantitative Fmoc substitution level was determined for the resin. Unreacted sites were capped by treating the resin with acetic anhydride (10 equiv) and DIEA (20 equiv) in DMF for 30 min if necessary. The reagents were drained, and the resin was washed with DMF, DCM, and DMF. Deprotection was carried out using 20% piperidine/DMF (2 × 15 min); the resin was then washed with DMF, DCM, and DMF. Subsequent Gly, Gly couplings were carried out using the above procedure over 4 h durations.

General Procedure for Synthesis of TFMPD-K(Cy3)-GGX-NHOH (5). Fmoc-Lys(Cy3)-OH **1** (4 equiv), TBTU (4 equiv), and HOBt (4 equiv) were dissolved in a minimal amount of DMF. DIEA (8 equiv) was added, and the mixture was shaken for 10 min. The solution was then added to the resin **4**, and the reaction mixture was agitated for 4 h, drained, and washed with DMF, DCM, and DMF. Fmoc deprotection of the resulting resin was carried out using 20% piperidine (in DMF; 2 × 15 min) to yield resin-bound H_2N-K(Cy3)-GGX-NHOH. Next, 20 mg of the resin were swelled in DMF for 1 h. 4-(3-Trifluoromethyl-3*H*-diazirin-3-yl)-benzoic acid (4 equiv), TBTU (4 equiv), and HOBt (4 equiv) were dissolved in a minimal amount of DMF. DIEA (8 equiv) was added, and the mixture was shaken for 10 min. The solution was then added to the resin, and the reaction mixture was agitated for 4 h in the dark. Subsequently, the resin was washed with DMF, DCM, and MeOH. The resulting product was cleaved from the solid support using a cleavage cocktail (95% TFA, 2.5% TIS(triisopropylsilane) and 2.5% water; 0.5 mL total volume) for 2 h. The filtered solution was subsequently concentrated in vacuo and purified by RP-HPLC to afford the final pure product. Using the above-described protocol, the following compounds were prepared (Table 1):

TFMPD-K(Cy3)-GGL-NHOH (5a). The compound was afforded as a red solid (6 mg; 37% yield): ^{1}H NMR (300 MHz, CD_3OD) δ 8.58 (dd, J = 13.7 Hz, J = 12.8 Hz, 1H), 7.95 (d, J = 8.0 Hz, 2H), 7.54−7.23 (m, 10H), 4.43−4.34 (m, 2H), 4.12 (br t, J = 6.8 Hz, 2H), 3.88−3.86 (m, 4H), 3.67 (s, 3H), 3.17 (m, 2H), 2.25 (br t, J = 6.6 Hz, 2H), 1.93−1.25 (m, 25H) including 1.76 (s, 6H) and1.75 (s, 6H), 0.92 (d, J = 5.2 Hz, 3H), 0.87 (d, J = 5.6 Hz, 3H); ^{19}F NMR (282 MHz, CD_3OD) δ −0.92; ESI-MS calcd for $C_{54}H_{68}F_3N_{10}O_7$ $[M - I]^+$ 1025.5, found 1025.4.

TFMPD-K(Cy3)-GGI-NHOH (5b). The compound was afforded as a red solid (4 mg; 22% yield): ^{1}H NMR (300 MHz, CD_3OD) δ 8.46 (dd, J = 13.3 Hz, 13.6 Hz, 1H), 7.88 (d, J = 8.4 Hz, 2H), 7.45 (d, J = 7.3 Hz, 2H), 7.39−7.33 (m, 2H), 7.28−7.19 (m, 6H), 6.35 (d, J = 13.6 Hz, 2H), 4.38−4.33 (m, 1H), 4.08−4.00 (m, 3H), 3.87−3.73 (m, 4H), 3.59 (s, 3H), 3.10 (t, J = 6.4 Hz, 2H), 2.17 (t, J = 6.6 Hz,

(12) While our manuscript was under review, Cravatt et al. independently reported a benzophenone-containing hydroxamate probe that targets metalloproteases specifically MMPs (Saghatelian, A.; Jessani, N.; Joseph, A.; Humphrey, M.; Cravatt, B. F. *Proc. Natl. Acad. Sci. U.S.A.* **2004**, *101*, 10000−10005).

(13) (a) Mellor, S. L.; McGuire, C.; Chan, W. C. *Tetrahedron Lett.* **1997**, *38*, 3311−3314. (b) Chan, W. C.; Mellor, S. L.; Atkinson, G. E. In *N-Fmoc-aminooxy-2-chlorotrityl polystyrene resin for High Throughput Synthesis of Hydroxamic Acids in Solid-Phase Organic Syntheses: Volume One*; Czarnik, A. W., Ed; John Wiley & Sons: 2001.

Table 1. Analogues of 4-(3-Trifluoromethyl)phenyldiazirine-K(Cy3)-GGX-hydroxamates Synthesized, Where X Represents the Amino Acid in the P_1 Position[a]

	amino acid /P_1 residue	yield %[a]
5a	Leu	37
5b	Ile	22
5c	Val	16
5d	Met	27
5e	Phe	18
5f	Gly	6
5g	Thr	38
5h	Lys	8
5i	Glu	16

[a] Yields were calculated based on an average of 0.80 mmol/g substitution level of hydroxylamine-functionalized resin **3**.

2H), 1.95−0.99 (m, 25H) including 1.68 (s, 6H) and 1.67 (s, 6H); ^{19}F NMR (282 MHz, CD_3OD) δ −0.95; ESI-MS calcd for $C_{54}H_{68}F_3N_{10}O_7$ $[M - I]^+$ 1025.5, found 1025.5.

TFMPD-K(Cy3)-GGV-NHOH (5c). The compound was afforded as a red solid (3 mg; 16% yield): ^{1}H NMR (300 MHz, CD_3OD) δ 8.46 (dd, J = 13.2 Hz, J = 13.6 Hz, 1H), 7.88 (d, J = 8.4 Hz, 2H), 7.46 (d, J = 7.3 Hz, 2H), 7.40−7.33 (m, 2H), 7.29−7.19 (m, 6H), 6.35 (d, J = 13.6 Hz, 2H), 4.35−4.30 (m, 1H), 4.19−4.13 (m, 1H), 4.06 (t, J = 7.0 Hz, 2H), 3.84−3.81 (m, 4H), 3.60 (s, 3H), 3.10 (t, J = 5.6 Hz, 2H), 2.17 (t, J = 6.4 Hz, 2H), 1.91−1.17 (m, 23H) including 1.68 (s, 6H) and 1.68 (s, 6H), 0.93−0.82 (m, 6H); ^{19}F NMR (282 MHz, CD_3OD) δ −1.11; ESI-MS cald for $C_{53}H_{66}F_3N_{10}O_7$ $[M - I]^+$ 1011.5, found 1011.4.

TFMPD-K(Cy3)-GGM-NHOH (5d). The compound was afforded as a red solid (5 mg; 27% yield): ^{1}H NMR (300 MHz, CD_3OD) δ 8.54 (dd, J = 13.6 Hz, J = 13.2 Hz, 1H), 7.97 (d, J = 8.4 Hz, 2H), 7.54 (d, J = 7.3 Hz, 2H), 7.48−7.42 (m, 2H), 7.37−7.28 (m, 6H), 6.44 (d, J = 13.6 Hz, 2H), 4.46−4.42 (m, 2H), 4.14 (t, J = 7.0 Hz, 2H), 3.90−3.87 (m, 4H), 3.68 (s, 3H), 2.56−2.41 (m, 2H), 2.26 (t, J = 6.6 Hz, 2H), 2.05−1.29 (m, 27H) including 2.05 (s, 3H), 1.77 (s, 6H), 1.76 (s, 6H); ^{19}F NMR (282 MHz, CD_3OD) δ −1.05; ESI-MS calcd for $C_{53}H_{66}F_3N_{10}O_7S$ $[M - I]^+$ 1043.5, found 1043.4.

TFMPD-K(Cy3)-GGF-NHOH (5e). The compound was afforded as a red solid (3 mg;18% yield): ^{1}H NMR (300 MHz, CD_3OD) δ 8.53 (dd, J = 13.2 Hz, J = 13.3 Hz, 1H), 7.96−7.89 (m, 2H), 7.72−7.60 (m, 1H), 7.53−7.19 (m, 14H), 6.41 (d, J = 13.3 Hz, 2H), 4.54−4.42 (m, 1H), 4.22−4.10 (m, 5H), 3.86−3.80 (m, 2H), 3.66 (s, 3H), 3.13 (br t, J = 5.6 Hz, 2H), 2.24 (br t, J = 6.6 Hz, 2H), 1.78−1.29 (m, 24H) including 1.75 (s, 6H) and 1.74 (s, 6H); ^{19}F NMR (282 MHz, CD_3OD) δ −0.78; ESI-MS calcd for $C_{57}H_{66}F_3N_{10}O_7$ $[M - I]^+$ 1059.5, found 1059.3.

TFMPD-K(Cy3)-GGG-NHOH (5f). The compound was afforded as a red solid (1 mg; 6% yield): ^{1}H NMR (300 MHz, CD_3OD) δ 8.57 (dd, J = 13.6 Hz, J = 13.2 Hz, 1H), 7.98 (d, J = 8.4 Hz, 2H), 7.56 (d, J = 7.3 Hz, 2H), 7.50−7.44 (m, 2H), 7.39−7.30 (m, 6H), 6.46 (d, J = 13.6 Hz, 2H), 4.49−4.45 (m, 1H), 4.16 (t, J = 6.6 Hz, 2H), 3.96−3.82 (m, 6H), 3.70 (s, 3H), 3.21 (t, J = 6.5 Hz, 2H), 2.28 (t, J = 6.6 Hz, 2H), 2.06−1.48 (m, 22H) including 1.79 (s, 6H) and 1.78 (s, 6H); ^{19}F NMR (282 MHz, CD_3OD) δ −1.30; ESI-MS calcd for $C_{50}H_{60}F_3N_{10}O_7$ $[M - I]^+$ 969.5, found 969.4.

TFMPD-K(Cy3)-GGT-NHOH (5g). The compound was afforded as a red solid (7 mg; 38% yield): ^{1}H NMR (300 MHz, CD_3OD) δ 8.46 (dd, J = 13.6 Hz, J = 13.2 Hz, 1H), 7.88 (d, J = 8.7 Hz, 2H), 7.46 (d, J = 7.3 Hz, 2H), 7.40−7.33 (m, 2H), 7.29−7.20 (m, 6H), 6.35 (d, J = 13.6 Hz, 2H), 4.38−4.34 (m, 1H), 4.16−4.13 (m, 2H), 4.08−4.04 (m, 2H), 3.86−3.80 (m, 3H), 3.60 (s, 3H), 3.16−2.99 (m, 3H), 2.17 (t, J = 6.4 Hz, 2H), 1.68−1.21 (m, 22H) including 1.68 (s, 6H) and 1.67 (s, 6H), 1.07 (d, J = 6.27 Hz, 3H); ^{19}F NMR (282 MHz, CD_3OD) δ −1.08; ESI-MS calcd for $C_{52}H_{64}F_3N_{10}O_8$ $[M - I]^+$ 1013.5, found 1013.4.

TFMPD-K(Cy3)-GGK-NHOH (5h). The compound was afforded as a red solid (2 mg; 11% yield): ^{1}H NMR (300 MHz, CD_3OD) δ 8.55 (dd, J = 13.6 Hz, J = 13.6 Hz, 1H)), 7.97 (d, J = 8.4 Hz, 2H), 7.54 (d, J = 7.3 Hz, 2H), 7.48−7.41 (m, 2H), 7.37 (m, 6H), 6.43 (d, J = 13.6 Hz, 2H), 4.44−4.30 (m, 2H), 4.14 (t, J = 6.8 Hz, 2H), 3.97−3.80 (m, 4H), 3.68 (s, 3H), 3.18 (t, J = 6.8 Hz, 2H), 2.92 (t, J = 7.5 Hz, 2H), 2.26 (t, J = 6.6 Hz, 2H), 1.77−1.29 including 1.77 (s, 6H) and 1.76 (s, 6H); ^{19}F NMR (282 MHz, CD_3OD) δ −1.24; ESI-MS calcd for $C_{54}H_{69}F_3N_{11}O_7$ $[M - I]^+$ 1040.5, found 1040.4.

TFMPD-K(Cy3)-GGE-NHOH (5i). The compound was afforded as a red solid (3 mg; 16% yield): ^{1}H NMR (300 MHz, CD_3OD) δ 8.54 (dd, J = 13.6 Hz, J = 13.2 Hz, 1H), 7.97 (d, J = 8.4 Hz, 2H), 7.54 (d, J = 7.3 Hz, 2H), 7.48−7.42 (m, 2H), 7.37−7.28 (m, 6H), 6.43 (d, J = 13.2 Hz, 2H), 4.48−4.43 (m, 1H), 4.35 = 4.31 (m, 1H), 4.14 (t, J = 6.8 Hz, 2H), 3.89 (m, 4H), 3.68 (s, 3H), 3.19 (t, J = 6.6 Hz, 2H), 2.40−2.35 (m, 2H), 2.26 (t, J = 6.5 Hz, 2H), 2.16−1.30 (m, 24H) including 1.77 (s, 6H) and 1.76 (s, 6H); ^{19}F NMR (282 MHz, CD_3OD) δ −0.95; ESI-MS calcd for ESI-MS calcd for $C_{53}H_{64}F_3N_{10}O_9$ $[M - I]^+$ 1041.5, found 1041.3.

BP-K(Cy3)-GGL-NHOH (6). Fmoc-Lys(Cy3)-OH **1** (4 equiv), TBTU (4 equiv), and HOBt (4 equiv) were dissolved in a minimal amount of DMF. DIEA (8 equiv) was added, and the mixture was shaken for 10 min. The solution was then added to the resin **4a** in the reaction vessel, and the reaction mixture was agitated for 4 h. Subsequently, the reagents were drained, and the resin was washed with DMF, DCM, and DMF. Fmoc deprotection was performed using 20% piperidine (in DMF; 2 × 15 min) to yield the resin-bound H_2N-K(Cy3)-GGL-NHOH. Next, 20 mg of the resin were swelled in DMF for 1 h. 4-Benzoylbenzoic acid (4 equiv), TBTU (4 equiv), and HOBt (4 equiv) were dissolved in a minimal amount of DMF. DIEA (8 equiv) was added, and the mixture was shaken for 10 min. The solution was then added to the resin, and the reaction mixture was agitated for 4 h in the dark. The resulting resin was washed with DMF, DCM, and MeOH. The product was cleaved from the resin using a cleavage cocktail (95% TFA, 2.5% TIS, and 2.5% water; 0.5 mL total volume) for 2 h. The filtered solution was subsequently concentrated in vacuo and purified with RP-HPLC to afford the final product, **6**, as a red solid (2.5 mg; 14% yield): ^{1}H NMR (300 MHz, CD_3OD) δ 8.52 (dd, J = 13.7 Hz, J = 13.2 Hz, 1H), 8.01 (d, J = 8.4 Hz, 2H), 7.83−7.74 (m, 4H), 7.67−7.62 (m, 1H), 7.54−7.49 (m, 4H), 7.47−7.40 (m, 2H), 7.35−7.26 (m, 4H), 6.41 (dd, J = 13.3 Hz, 13.3 Hz, 2H), 4.52−4.46 (m, 1H), 4.37−4.32 (m, 1H), 4.11 (t, J = 6.8 Hz, 2H), 3.91−3.89 (m, 4H), 3.20 (t, J = 6.4 Hz, 2H), 2.25 (t, J = 6.6 Hz, 2H), 1.98−1.45 (m, 25H) including 1.75 (s, 6H) and 1.74 (s, 6H), 0.90 (dd, J = 6.0 Hz, J = 6.0 Hz, 6H); ESI-MS calcd for ESI-MS calcd for $C_{59}H_{73}N_8O_8$ $[M - I]^+$ 1021.6, found 1021.6.

TFMPD-K(Biotin)-GGL-NHOH (7). The H_2N-GGL-hydroxamate-functionalized resin (20 mg) was preswelled in DMF for 1 h. Separately, Fmoc-Lys(Biotin)-OH (4 equiv), TBTU (4 equiv), and HOBt (4 equiv) were dissolved in a minimal amount of DMF. DIEA (8 equiv) was subsequently added, and the mixture was shaken for 10 min and then added to the resin. The resulting mixture was agitated for 4 h. The resin was washed with DMF, DCM, and DMF. Fmoc deprotection was performed using 20% piperidine (in DMF; 0.5 mL) for 30 min, after which the resin was washed with DMF, DCM, and DMF. A preactivated solution of 4-(3-trifluoromethyl-3*H*-diazirin-3-yl)benzoic acid (4 equiv), TBTU (4 equiv), HOBt (4 equiv), and DIEA (8 equiv) was subsequently added. The solution was agitated for 4 h and drained, and the resulting resin was washed twice with DMF, DCM, and MeOH before drying in vacuo overnight. The resin-bound product was cleaved using a cleavage cocktail (95% TFA, 2.5% TIS, and 2.5% water; 0.5 mL total volume) for 2 h. The filtered solution was subsequently concentrated in vacuo and purified with RP-HPLC to afford the desired product as a white solid (2.0 mg; 15% yield): ^{1}H NMR (300 MHz, CD_3OD) δ 7.98 (d, J = 8.4 Hz, 2H), 7.35 (d, J = 8.4 Hz, 2H), 4.50−4.42 (m, 2H), 4.37−4.26 (m, 2H), 3.97−3.83 (m, 4H), 3.34 (m, 1H), 2.91 (dd,

J = 5.0 Hz, J = 12.7 Hz, 1H), 2.71−2.62 (m, 1H), 2.17 (t, J = 7.1, 2H), 2.02−1.38 (m, 15H), 0.93 (d, J = 5.9 Hz, 3H), 0.89 (d, J = 6.3 Hz, 3H);^{19}F NMR (282 MHz, CD_3OD) δ −1.27; ESI-MS calcd for $C_{35}H_{50}F_3N_{10}O_8S$ $[M + H]^+$ 827.3, found 827.3.

GGL-NHOH (8). 100 mg of resin-bound GGL-NHOH **4a** was cleaved off using a cleavage cocktail of TFA/TIS/water (95:2.5:2.5). The solution was triturated in cold ether, and the resulting precipitate was collected, washed repeatedly with cold ether, lyophilized and purified by RP-HPLC to afford **8** as a white solid, (10 mg; 48% yield). ESI-MS cald for $C_{10}H_{21}N_4O_4$ $[M+H]^+$ 261.2, found 261.0.

Preparation of Positional-Scanning Libraries of Hydroxamate-Based Metalloprotease Inhibitors. The synthesis was carried out using standard positional-scanning protocols, as reported previously.[14] A mixture of 18 amino acids (20 standard amino acids, minus Cys and Tyr) was used in position X. Hydroxamate-functionalized resin (2 g, 0.80 mmol/g) with Leu in the P_1 position was prepared as described above. Fmoc deprotection steps were performed using 20% piperidine (in DMF) for 30 min. Subsequent peptide coupling steps were carried out in a 96-well block reactor system (FlexChem, USA). Briefly, resin-bound Leu-NHOH (50 mg) was weighed into each well. Preactivated solutions of Fmoc-amino acids (4 equiv), HBTU (4 equiv), HOBt (2-(1-*H*-benzotriazol-1-yl)-1,1,3,3-tetramethyluronium hexafluorophosphate) (4 equiv), and DIEA (8 equiv) were added into each well, and the reaction mixtures were agitated for 6 h. Reagents were drained, and the resin was washed with DMF, DCM, and DMF. Subsequent Fmoc deprotection and coupling steps were carried out similarly. Double couplings were done, if necessary, throughout the peptide synthesis. The final wash of the resin was carried out with MeOH, and the resin was dried in vacuo overnight. Cleavage of the peptide from the resin was carried out with a cleavage cocktail consisting of TFA/thioanisole/anisole/EDT (90/5/3/2; 2 mL) for 2 h. The filtrate was triturated in cold ether. The precipitated peptides were collected, washed repeatedly with cold ether, and dried in vacuo. Finally, the solid was dissolved in water, lyophilized, and used without further purifications.

Enzyme Labeling Studies. Unless otherwise stated, all enzymes used for labeling studies were purchased from commercial suppliers. Stock solutions of enzymes were prepared in final concentrations of 5−10 mg/mL (in H_2O) and stored at −20 °C. Desalted stock solutions were prepared, if necessary, by passing the above enzyme solutions through an NAP5 desalting column (Amersham, USA) prior to use. Stock solutions of the probes were prepared in DMSO (dimethyl sulfoxide) and stored at −20 °C until use. UV photolysis experiments were carried out using a handheld UV lamp (UVP, USA). Fluorescence imaging was performed using a Typhoon 9200 fluorescence gel scanner (Amersham, USA) at λ_{ex} = 532 nm and analyzed with the ImageQuant software (Amersham, USA).

General Procedure for Photoaffinity Labeling Studies. Unless otherwise stated, 2 μL of an enzyme stock solution (5−10 mg/mL) were diluted with 17.8 μL of Tris·HCl buffer (50 mM, pH 8). The probe stock solution (0.2 μL, 50 μM in DMSO) was added, and the reaction was incubated at room temperature in the dark for 30 min. Subsequently, the reaction mixture was irradiated with a handheld UV lamp under the long-range UV channel for 20 min. The reaction was quenched by the addition of 4 μL of 6 × SDS loading buffer followed by boiling at 95 °C for 10 min. Samples were analyzed on a 12% denaturing SDS-PAGE gel, and fluorescence was detected with the Typhoon fluorescence gel scanner.

A. Concentration-Dependent Labeling Studies. A 2 μL aliquot of thermolysin stock solution (10 mg/mL) was diluted with 17.8 μL of Tris·HCl buffer (50 mM, pH 8). A 0.2 μL aliquot of the probe (2 mM, 500, 200, 100, 50, 20, 10, 5, 2, and 1 μM DMSO) was added. A reaction having the enzyme alone in Tris·HCl buffer was also set up as a negative control. The samples were then treated as mentioned above. To determine the detection limit of the probe **5a**, the 500 nM the probe was incubated with varied amounts of the enzyme (thermolysin: 1000, 100, 50, 30, 10, 5, 1 ng. MMP-9: 100, 10, 1, 0.1 ng) in a 20 μL reaction.

B. Labeling Experiments with Variable Irradiation Time. A 2 μL aliquot of the thermolysin stock solution (10 mg/mL) was diluted with 17.8 μL of Tris·HCl buffer (50 mM, pH 8). A 0.2 μL aliquot of probe (50 μM) was added, and the reactions were incubated at room temperature in the dark for 30 min. The reaction mixtures were then irradiated for 0, 10, 20, 30, and 60 min with UV light, quenched, and analyzed by SDS-PAGE as described above.

C. Heat-Denaturing Experiments. A 2 μL aliquot of thermolysin solution (10 mg/mL) was diluted with 17.8 μL of Tris·HCl buffer (50 mM, pH 8). The solution was heated at 95 °C for 10 min and allowed to cool to room temperature. A 0.2 μL aliquot of the probe (50 μM in DMSO) was added, and the reaction was incubated at room temperature in the dark for 30 min, irradiated under UV for 20 min, and analyzed as described above.

C. Dose-Dependent Inhibition Studies. Please refer to the Supporting Information for more details. Briefly, 2 μL of thermolysin solution (100 ng/μL) were diluted with 18 μL of Tris·HCl buffer (50 mM, pH 8). For GGL-NHOH inhibition, 0, 10, 100, 1000, 10^4, 10^5, 5 × 10^5, 10^6, and 5 × 10^6 nM concentrations of the inhibitor were used. For GM6001 inhibition, 0, 1.3, 6.5, 10, 13, 65, 100, 130, 260, 500, and 1000 nM concentrations of the inhibitor were used. A 2 μL aliquot of a desired inhibitor, with varied concentrations (dissolved in H_2O, with or without <10% DMSO depending on the solubility of the inhibitor), was added, followed by 0.2 μL of the probe, **5a** (50 μM in DMSO; final concentration in the reaction, 500 nM). The reaction was incubated at room temperature in the dark for 15−30 min, irradiated under UV for 20 min, and analyzed as described above. The fluorescent bands were quantitated, and the IC_{50} of the inhibitor was calculated by fitting the resulting dose-dependent data with the PRISM software (GraphPad, USA). Dose-dependent inhibition studies with the positional scanning (PS) libraries were performed similarly and summarized in Figure 3c.

D. EDTA Inhibition Studies. A 2 μL aliquot of the desalted thermolysin stock solution (5 mg/mL) was diluted with 15.8 μL of Tris·HCl buffer (50 mM, pH 8). A 2 μL aliquot of an EDTA (*N*,*N*,*N*′,*N*′-ethylenediaminetetraacetic acid) stock solution (0, 100, 500, and 1000 μM in water, pH 8) and a 0.2 μL aliquot of the probe (50 μM in DMSO) were added simultaneously. The reaction was incubated at room temperature in the dark for 30 min, irradiated under UV for 20 min, and analyzed as described above.

Labeling of Thermolysin Spiked in Yeast Cell Extract. For spike experiments with the probe **5a**, the amount of thermolysin was kept constant while the concentration of the yeast extract was varied. Briefly, 200 ng of thermolysin were added to yeast extracts which contain varied amounts of total yeast proteins (0, 8, 20, 40, 80, 160, 320, and 640 μg, respectively). The resulting extracts (final volume upon addition of buffer: 20 μL) were labeled with **5a** (final concentration: 5 μM) for 20 min. For comparison between the two probes, 10 μg of thermolysin, both in pure form and spiked in the yeast extract (contains 100 μg of total proteins), were labeled with **5a** and **6** (final concentration: 5 μM). All reactions were analyzed by SDS-PAGE followed by both fluorescence scanning and Coomassie staining.

Labeling of Yeast Metalloproteases. The yeast metalloproteases were expressed from *S. cerevisiae* using the ExClone Yeast ORF expression clones (Invitrogen),[15] which contain different yeast open reading frames (ORF) fused to glutathione-*S*-transferase (GST). The GST-fusion constructs have been cloned under the copper-inducible Pcup1 promoter. For protein expression, an overnight culture of the yeast having the desired ORF and grown in uracil-deficient minimal media supplemented with 20% glucose was diluted 1:50 into minimal media lacking uracil and leucine. The culture was then grown until

(14) Uttamchandani, M.; Chan, E. W. S.; Chen, G. Y. J.; Yao, S. Q. *Bioorg. Med. Chem. Lett.* **2003**, *13*, 2997−3000.

(15) www.invitrogen.com

$OD_{600} = 0.8$, at which point 0.5 mM $CuSO_4$ was added to induce protein expression. After induction of expression for 2 h at 30 °C, cells were spun down, resuspended in lysis buffer (50 mM Tris·HCl, pH 8.0, 100 mM NaCl, 0.1% Triton X-100), and lysed by mechanical disruption using 400−625 micron diameter glass beads (Sigma) in a bead mill at 30 Hz for 10 min (Retsch Instruments). The lysate was clarified by centrifugation at 13 000 rpm for 10 min, and the final protein concentration was adjusted to 10 mg/mL. For protein purification, 400 μL of the cell lysate were applied to a MicroSpin GST column (Amersham, USA) containing Glutathione Sepharose 4B and incubated at 4 °C for 1 h with gentle agitation, followed by extensive washing with lysis buffer to reduce nonspecific bindings. The resulting purified protein, still bound to the beads, was incubated with a desired probe (final probe concentration: 5 μM) in 50 mM Tris (pH 8.0) for 1 h. UV irradiation and SDS-PAGE analysis was done as mentioned above. For immunoblotting experiments, the proteins resolved on SDS-PAGE were transferred to PVDF (polyvinylidene fluoride) membranes, probed with anti-GST antibodies, and detected by chemiluminescence using the ECL plus kit (Amersham, USA) according to the manufacturer's instructions.

Results and Discussion.

Design of Photoactive Affinity Probes for Metalloproteases. Metalloproteases are a class of hydrolytic enzymes belonging to the protease family.[16] Major metalloproteases, such as the matrix metalloproteinases (MMPs) and angiotensin-converting enzymes (ACE),[17,18] have been shown to actively participate in a number of physiological pathways, such as tissue modeling and blood pressure regulation, rendering them potential pharmaceutical targets in diseases such as arthritis,[19] Alzheimer's disease,[20] cancer,[21] and heart disease.[22] These enzymes, through a catalytic zinc(II) ion coordinated to three amino acid residues (usually His and Glu) and a water molecule located within the enzyme active site, hydrolyze peptide bonds via a general-base mechanism. During the hydrolysis, the tetrahedral peptide intermediate formed is coordinated to zinc but not covalently bound to the enzyme.[23] Consequently, no mechanism-based, irreversible inhibitors of these enzymes are currently known, making it impossible, using existing strategies,[7,8] to develop suitable chemical probes for activity-based profiling experiments.

To develop techniques which allow large-scale identification of novel metalloproteases present in a proteome, we searched for chemical functionalities which possess high-affinity binding to these enzymes by capitalizing on the rich history of enzyme-inhibition studies. The majority of metalloprotease inhibitors are substrate-based analogues that contain zinc-binding groups (ZBGs), which, within the active site of the enzyme, compete with water for the binding to the catalytically active zinc ion, thereby preventing the hydrolytic action from taking place.[23] Known ZBGs include formyl hydrazines, sulfhydryls, and aminocarboxylates, but the most potent of ZBGs are the hydroxamic acids,[23,24] which chelate zinc through their carboxyl and hydroxyl oxygens (Figure 1b, c).

In our design, we selected peptide-based hydroxamate inhibitors for the affinity binding to metalloproteases (Scheme 1).[23b,25] By using a simplistic model, we made probes having GGX-NHOH sequences, in which X represents the P_1 residue, thus encoding the sole substrate recognition unit and rendering them useful for potential broad-based profiling of metalloproteases. Two glycine residues were inserted at the P_2 and P_3 positions to serve as a flexible linker that extends the ZBG away from the fluorophore/biotin and the photolabile group in the probes, thus minimizing their potential interference, if any, when binding to the active site of the enzyme. Diazirine was selected as the photolabile group of choice. The C−N bond of 3-trifluoromethyl-3-phenyldiazirine cleaves homolytically at 360 nm to yield a triplet carbene that inserts into any C−H bonds in the vicinity of the reactive species.[10a−e] In the recent report by Hagenstein et al., benzophenone was selected as the photolabile group for protein cross-linking.[11] We therefore synthesized a benzophenone-tagged probe, **6**, for the synchronous comparison with our diazirine-based probes (vide infra; see Scheme 1).[12] A cyanine dye, Cy3, as well as biotin, was chosen as the reporter tag for easy detection and enrichment of labeled proteins, respectively. The three key components were assembled together using lysine as a trifunctional handle.

Chemical Synthesis of Probes and Inhibitors (Scheme 1). The peptidyl hydroxamate probes were synthesized by standard Fmoc solid-phase peptide synthesis protocols using hydroxylamine-functionalized 2-chlorotrityl chloride resin **3**, synthesized as previously reported.[13] The GGX tripeptidyl sequence was loaded onto the resin **3** using TBTU-activated coupling protocols where X denotes the amino acid of choice for the P_1 position. The following steps involved the anchoring of the fluorophore Cy3 onto the trifunctional lysine molecule. Cy3 was converted to its corresponding NHS (*N*-hydroxysuccinimide) ester and then coupled to the ϵ-amino group of Fmoc-Lys-OH to yield **1**, Fmoc-Lys(Cy3)-OH, which was then coupled onto the resin-bound GGX-hydroxamate using standard solid-phase peptide synthesis protocols. Following Fmoc deprotection, the diazirine moiety was coupled to the α-amino group of lysine in the final step of the synthesis. Cleavage of the substrate from the solid support using 95% TFA followed by preparative RP-HPLC purification gave the desired products. Using the described method, we synthesized nine hydroxamate-based affinity probes with varied P_1 residues: hydrophobic (Leu **5a**, Ile **5b**, Val **5c**, Met **5d**); aromatic (Phe **5e**); hydrophilic (Gly **5f**, Thr **5g**); basic (Lys **5h**); and acidic (Glu **5i**). The benzophenone- and biotin-containing probes, **6** and **7**, were similarly synthesized.

A positional-scanning inhibitor library of peptidyl hydroxamates having Leu at the P_1 position was synthesized to investigate the substrate specificity of metalloproteases at the P_2-P_4 positions. An array of 8 representative amino acids was selected to individually "scan" through the P_2-P_4 positions in each library, and they are Ala, Glu, Phe, Lys, Leu, Pro, Gln and Ser. The positional-scanning libraries were synthesized on a 96-well reactor block system using HBTU-mediated Fmoc peptide coupling protocols,[14] resulting in a total of 24 peptide hydroxamate libraries.

(16) Hooper, N. M. *FEBS Lett*. **1994**, *354*, 1−6.
(17) Bode, W.; Maskos, K. *Biol. Chem*. **2003**, *384*, 863−872.
(18) Turner, A. J. *Biochem. Soc. Trans*. **2003**, *31 (Pt 3)*, 723−727.
(19) Martel-Pelletier, J.; Welsch, D. J.; Pelletier, J. P. *Best Pract. Res. Clin. Rheumatol*. **2001**, *15*, 805−829.
(20) Hooper, N. M.; Turner, A. J. *Curr. Med. Chem*. **2002**, *9*, 1107−1119.
(21) Vihinen, P.; Kahari, V. M. *Int. J. Cancer* **2002**, *99*, 157−166.
(22) Sierevogel, M. J.; Pasterkamp, G.; de Kleijn, D. P.; Strauss, B. H. *Curr. Pharm. Des*. **2003**, *9*, 1033−1040.
(23) (a) Whittaker, M.; Floyd, C. D.; Brown, P.; Gearing, A. J. H. *Chem. Rev*. **1999**, *99*, 2735−2776. (b) Skiles, J. W.; Gonnella, N. C.; Jeng, A. Y. *Curr. Med. Chem*. **2001**, *8*, 425−474.
(24) Muri, E. M.; Neito, M. J.; Sindelar, R. D.; Williamson, J. S. *Curr. Med. Chem*. **2002**, *9*, 1631−1653.
(25) Beckett, R. P.; Davidson, A. H.; Drummond, A. H.; Huxley, P.; Whittaker, M. *Drug Discuss. Today* **1996**, *1*, 16−26.

Scheme 1. Synthesis of Tripeptidyl Hydroxamate Inhibitors of Metalloproteases[a]

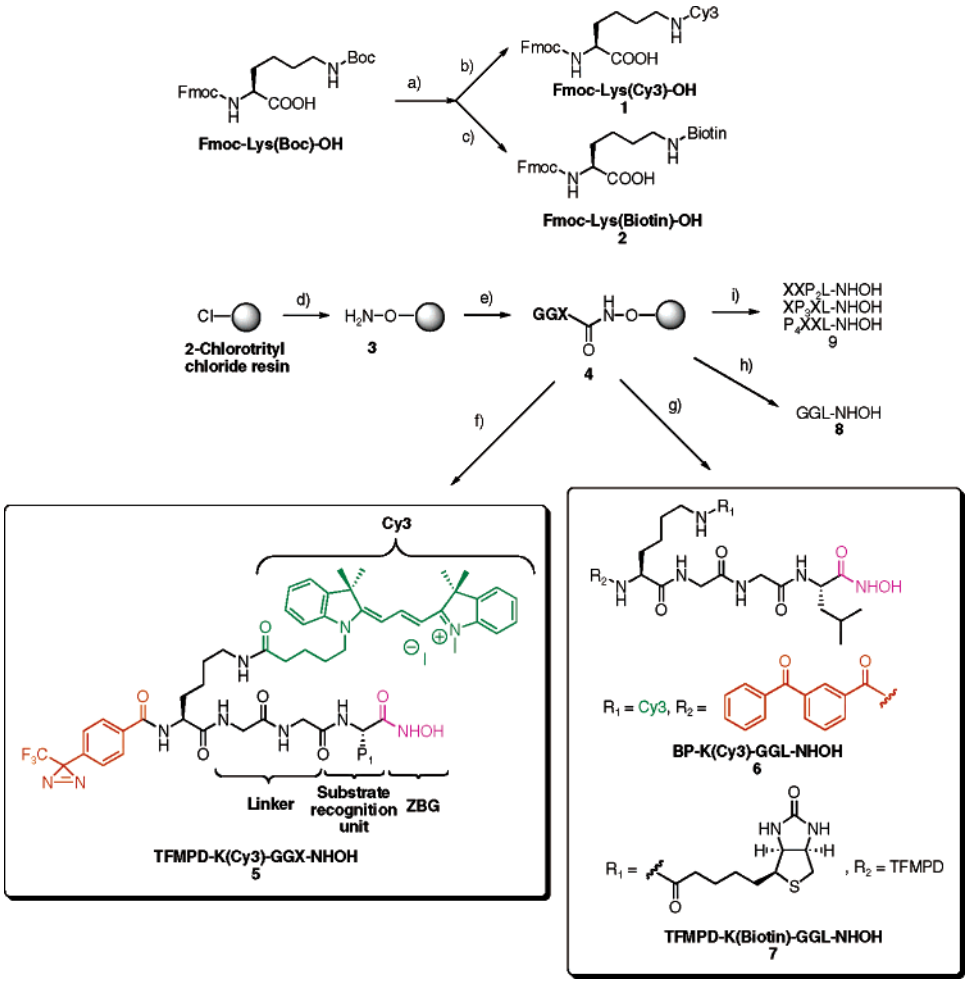

[a] (a) 50% TFA/DCM; (b) Cy3-NHS, DIEA, overnight; (c) biotin-NHS, DIEA, overnight; (d) (i) Fmoc-NHOH, DIEA, DCM, 48 h; (ii) 20% piperidine/DCM, 30 min; (e) (i) Fmoc-amino acid, TBTU, HOBt, DIEA; (ii) 20% piperidine/DMF; (f) (i) Fmoc-Lys(Cy3)-OH **1**, TBTU, HOBt, DIEA; (ii) 20% piperidine/DMF; (iii) TFMPD, TBTU, HOBt, DIEA; (iv) 95:2.5:2.5 TFA/TIS/H_2O; (g) (i) Fmoc-Lys(Cy3)-OH **1** or Fmoc-Lys(Biotin)-OH **2**, TBTU, HOBt, DIEA; (ii) 20% piperidine/DMF; (iii) TFMPD or 4-benzoyl benzoic acid, TBTU, HOBt, DIEA; (iv) 95:2.5:2.5 TFA/TIS/H_2O; (h) 95:2.5:2.5 TFA/TIS/H_2O; (i) (i) Fmoc-amino acids, HBTU, HOBt, DIEA; (ii) 20% piperidine/DMF; (iii) 90:5:3:2 TFA/thioanisole/anisole/EDT.

Optimization of Enzyme Labeling Conditions. Thermolysin, a 35 kDa extracellular endopeptidase isolated from *Bacillus thermoproteolyticus*, was selected as the model metalloprotease in our labeling experiments.[25,26] It is well documented that the enzyme favors a hydrophobic residue (e.g., Ile, Leu, or Val) at the P_1' position of its substrates.[27] Z-GGL-NHOH (Z, carbobenzyloxy) was previously shown to be a good inhibitor of thermolysin, with a K_i value of 39 μM.[28] X-ray crystallographic studies of the enzyme−inhibitor complex suggested that the GGL tripeptide binds inversely to the active site of the enzyme, with Leu fitting into the S_1' subsite.[29] We therefore chose the GGL-containing probe, **5a**, to investigate the efficacy of the labeling strategy toward thermolysin.

To determine the optimal probe concentration needed for efficient and specific labeling of thermolysin, stock solutions of **5a** with varying concentrations were prepared in DMSO. Different labeling reactions were set up, by varying the probe concentration while keeping the amount of thermolysin constant (final concentrations: probe = 0−20 μM; thermolysin = 20 μg). Control experiments were run using selected enzymes not belonging in the metalloprotease class. As shown in Figure 2a, specific labeling of thermolysin was observed when the probe concentration was greater than 50 nM. With increasing concentrations of the probe in the reaction, concurrent increases in the fluorescence intensity of the labeled thermolysin were observed. No labeling was observed for any of the control proteases when a low concentration of the probe was used (up to 1 μM final concentration). When higher concentrations of the probe were used, however, nonspecific labeling began to appear with control enzymes, giving rise to false positive results (Figure 2a). We thus determined the optimal concentration of the probe required for the specific labeling of thermolysin to be ~500 nM. This concentration was used for all subsequent labeling experiments, unless otherwise indicated.

We next determined the optimal UV irradiation time for the specific labeling of thermolysin. The labeling reaction with thermolysin was set up, in which 500 nM of the probe **5a** was

(26) Matthews, B. W. *Acc. Chem. Res.* **1988**, *21*, 333−340.
(27) Eijsink, V. G.; Veltman, O. R.; Aukema, W.; Vriend, G.; Venema, G. *Nat. Struct. Biol.* **1995**, *2*, 374−379.
(28) Holmes, M. A.; Matthews, B. W. *Biochemistry* **1981**, *20*, 6912−6920.
(29) Beynon, R. J.; Beaumont, A. Thermolysin. In *Handbook of Proteolytic Enzymes*; Barrett, A. J., Rawlings, N. D., Woessner, J. F., Eds.; Academic Press: 1998; p 1037.

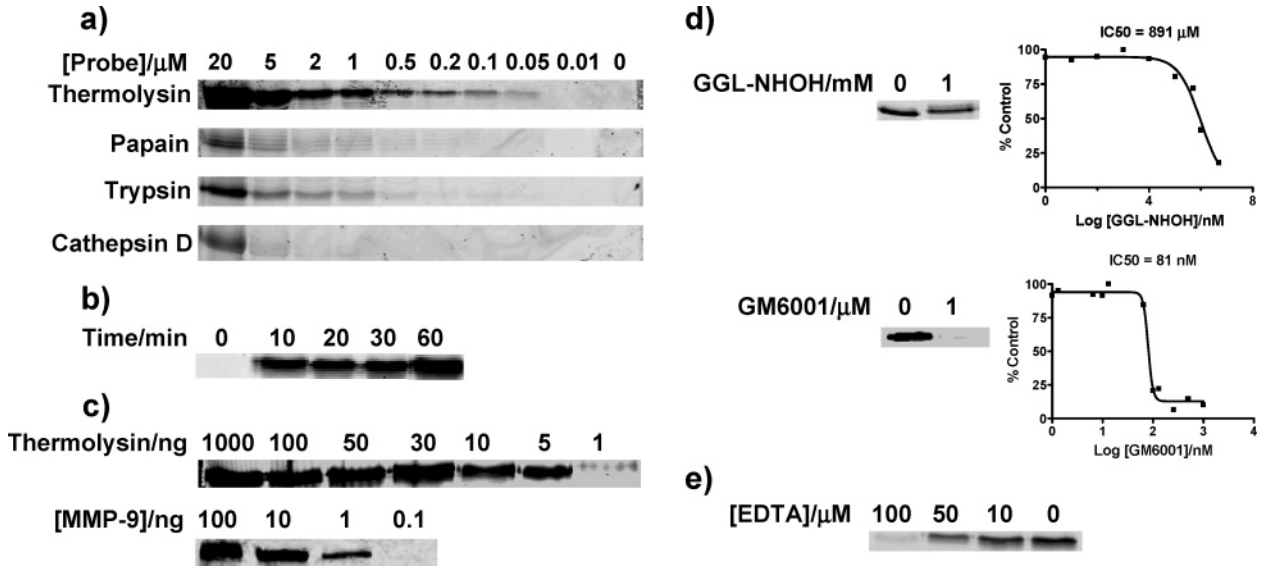

Figure 2. (a) Effect of probe concentration on labeling intensity: thermolysin and three other control enzymes (20 μg each), papain (cysteine protease), trypsin (serine protease), and cathepsin D (aspartic protease), were incubated with decreasing concentrations of **5a** (final concentration 20, 5, 2, 1, 0.5, 0.2, 0.1, 0.05, 0.01, and 0 μM, respectively); (b) effect of period of irradiation on labeling intensity: thermolysin (20 μg) incubated with **5a** (500 nM) was exposed to UV light for varying amounts of time (0, 10, 20, 30, and 60 min, respectively); (c) effect of enzyme concentration on labeling intensity: decreasing concentrations of thermolysin (1000, 100, 50, 30, 10, 5, and 1 ng, respectively) and MMP-9 (100, 10, 1, and 0.1 ng, respectively) were incubated with **5a** (final concentration: 500 nM); (d) competitive labeling experiments: thermolysin (200 ng) was incubated with **5a** (final concentration: 500 nM) and increasing amounts of GGL-NHOH **8** (0, 10, 100, 1000, 10^4, 10^5, 5×10^5, 10^6, and 5×10^6 nM, respectively; top panel) and GM6001 (0, 1.3, 6.5, 10, 13, 65, 100, 130, 260, 500, and 1000 nM, respectively; bottom panel). (Left) Shown is representative labeling of thermolysin by **5a** with and without the inhibitor. (Right) Shown is the dose-dependent inhibition of the labeling. (e) Competitive EDTA experiments. Desalted thermolysin was simultaneously incubated with **5a** (500 nM) and decreasing concentrations of EDTA (100, 50, 10, and 0 μM, respectively). See Supporting Information for further details.

used. Following incubation in the dark for 30 min, the reaction was UV irradiated for different lengths of time (0 to 60 min). As shown in Figure 2b, in the absence of photolysis, no labeling of thermolysin was observed, indicating that UV photolysis is essential for the labeling strategy. A concurrent increase in the thermolysin labeling was observed when the UV irradiation time increased from 0 to 60 min. Strong labeling was observed with as little as 10 min of irradiation time. We thus chose 20 min as the optimal time for UV irradiation in all subsequent experiments.

The sensitivity of the probe **5a** was next examined by incubating this reagent with a serial dilution of thermolysin, as well as a known matrix metalloprotease, MMP-9 (Figure 2c). Results indicated that **5a** could detect as little as 5 ng and 1 ng of pure thermolysin and MMP-9, respectively, approximating the detection limits of other known activity- and affinity-based probes.[7,8,11,12]

Mechanistic Studies of Thermolysin Labeling. Since one of the prerequisites for our labeling strategy is the presence of a functionally active site in the enzyme for the probe to bind before photo-labeling can occur, the extent of the enzyme labeling by a given probe can therefore be used to indirectly reflect the relative enzymatic activity of the enzyme, as well as the relative affinity of the probe against the enzyme, or both. A number of experiments were carried out to ensure that thermolysin labeling by **5a** depends on the probe's binding affinity toward the active site of the enzyme. First, competitive experiments were run, in which the labeling of thermolysin by **5a** was performed in the presence of a competitive inhibitor, **8**, which has the same **GGL-NHOH** binding unit as **5a**, but devoid of both the fluorescent and the photolabile units. This was further justified in the labeling of thermolysin (e.g., with **5a**) in the presence of GM6001, a highly potent, broad-spectrum metalloprotease inhibitor. EDTA, a well-known metal chelator which inhibits metalloproteases by removing their bound metals, was also tested in our labeling reactions. Finally, eight other probes, **TFMPD-K(Cy3)-GGX-NHOH**, **5b**−**5i**, in which X represents substitutions of different P_1 residues into the enzyme recognition sequence of the probe, were synthesized and tested against thermolysin, which, as an enzyme favoring hydrophobic P_1' residues, should confer different degrees of labeling by the probes (which bind the enzyme inversely).

GM6001, a highly potent hydroxamate-based metalloprotease inhibitor, is commercially available. GGL-NHOH, **8**, was obtained by TFA cleavage of the resin **4a** (Scheme 1) and lyophilized before use. Because hydroxamates are reversible inhibitors of metalloproteases, the presence of GM6001 or **8** in the labeling reaction of thermolysin with **5a** (final concentration: 500 nM) should competitively inhibit the labeling of the enzyme. This is evident in the dose-dependent inhibition experiments, as shown in Figure 2d, where the labeling of thermolysin by **5a** diminished in the presence of both **8** and GM6001, which blocked this reaction with IC_{50} values of 891 μM and 81 nM, respectively. These values agreed closely with microplate-based inhibition experiments (Supporting Information). The roughly 20-fold decrease in the inhibition of thermolysin by GGL-NHOH, as compared with the known Z-GGL-NHOH (K_i = 39 μM; see ref 28), may be caused by the removal of the hydrophobic carbobenzyloxy group in **8**.

EDTA is a well-known metal chelator, which inhibits a variety of metalloproteases by chelating to their catalytic metals. In the case of thermolysin, it was shown previously that EDTA inhibits the enzymatic activity of thermolysin by removing its active site-bound zinc ion involved in enzyme catalysis.[29] In our experiment, we studied the effect of EDTA on the enzyme labeling reaction. Desalted thermolysin was simultaneously

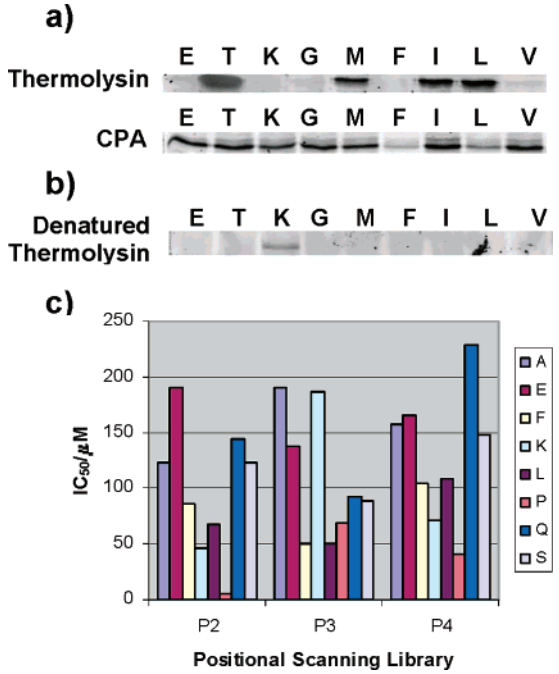

Figure 3. (a) Specificity profile of thermolysin and carboxypeptidase A. The enzymes (20 μg) were incubated with equal concentrations of the probes **5a**−**i** (final concentration: 500 nM); (b) hydroxamate probes (final concentration: 500 nM) against denatured thermolysin (20 μg); (c) plot of IC_{50} values from dose-dependent inhibition experiments of thermolysin (200 ng) labeling by **5a** (500 nM) in the presence of varying concentrations of peptides from the positional scanning library. For full details of results, see Supporting Information.

incubated with the photoaffinity probe (e.g., **5a**; final concentration: 500 nM) and varying concentrations of EDTA (Figure 2e). With increasing amounts of EDTA added to the reaction, fluorescence intensity of the labeled enzyme gradually decreased until the labeling was completely inhibited with 100 μM EDTA.

Asides from its preference for hydrophobic residues at the P_1' position, thermolysin was previously shown to exhibit some hydrolytic activity against substrates with hydrophilic P_1' side chains, such as Glu, Thr, and Lys.[30] We therefore synthesized eight more probes, **TFMPD-K(Cy3)-GGX-NHOH (5b-5i)**, having varied P_1 residues (representing P_1' positions when bound inversely to thermolysin). Together with **5a**, all nine probes were tested for their photoaffinity labeling against thermolysin, as well as carboxypeptidase A, another metalloprotease having a different substrate specificity profile. In addition, control labeling experiments were also performed with a number of nonmetalloproteases (data not shown). As shown in Figure 3a, it is evident that thermolysin exhibited intense labeling with peptidyl hydroxamates containing Thr, Met, Ile, and Leu at the P_1 position. Other probes bearing Glu, Lys, Gly, Phe, and Val residues at the P_1 position did not appreciably label the enzyme. Carboxypeptidase A, an exopeptidase that cleaves C-terminal residues from its peptide substrate, favors P_1' residues having branched aliphatic or aromatic residues (e.g., Tyr, Phe, Ile, and Leu).[27] Upon incubation with the nine hydroxamate probes, moderate labeling was observed for carboxypeptidase A with the majority of the probes, indicating the enzyme has little preference for residues at the P_1 position. We next used the probes to label heat-denatured thermolysin. The enzyme was first boiled at 95 °C for 10 min and then treated with the nine probes as described above (Figure 3b): no labeled thermolysin was observed with any of the probes, except **5h**, further confirming that a functional active site in the enzyme is essential for the labeling strategy to work. This feature is echoed by results obtained from control experiments in which nonmetalloproteases were used in the labeling experiments (data not shown): there was a complete absence of labeling in the control enzymes, further suggesting the specificity of the hydroxamate-containing probes is solely for metalloproteases. The faint labeling of denatured thermolysin with **5h** (e.g., the probe having Lys at the P_1 position), as shown in Figure 3b, may be due to some nonspecific labeling of the probe. The exact cause is still under investigation.

Positional-Scanning (PS) Libraries of Metalloprotease Inhibitors. We next assessed whether our affinity-based labeling approach could be used to screen for potential metalloprotease inhibitors in a gel-based format. Previously, Cravatt et al. had showed that activity-based profiling approaches were suitable for in situ screening of potential enzyme inhibitors.[31] We therefore tested the thermolysin labeling, by **5a**, in the presence of positional-scanning hydroxamate inhibitor libraries having XXP_2L-NHOH, XP_3XL-NHOH, and P_4XXL-NHOH sequences, in which P_2−P_4 represent individual amino acids of each inhibitor library being systematically substituted, or "scanned", at their respective P_2 to P_4 positions. Eight representative amino acids (e.g., Ala, Glu, Phe, Lys, Leu, Pro, Gln and Ser) were chosen to be individually "scanned" from P_2 through P_4 positions, so as to identify the preferred residues at each position. X represents a position in the inhibitor library having a mixture of 18 amino acids (20 standard amino acids, minus Cys and Tyr).[14] Leucine, the residue preferred by thermolysin at the P_1' position, was unaltered in the inhibitor libraries. In all, a total of 24 individually "scanned" libraries were synthesized and tested. Dose-dependent inhibition experiments were carried out as described above, where the thermolysin labeling reaction with **5a** was performed in the presence of different concentrations of each PS member, and the extent of labeling was compared and internally calibrated with control experiments in which no inhibitors were added (Supporting Information). Results were summarized, in which IC_{50} values of each PS member were compared (Figure 3c): all 24 hydroxamates showed a good inhibitory activity against thermolysin, with more potent inhibitors consistently possessing hydrophobic residues at P_2−P_4 positions (i.e., Pro and Leu). If one assumes the PS peptides bind inversely to the active site of thermolysin like other hydroxamate-based inhibitors (e.g., Z-GGL-NHOH; see ref 29), our results thus agree well with previous reports that thermolysin prefers hydrophobic amino acids at their P_2'−P_4' positions. Putting together these results indicates that the affinity-based labeling approach may be extended to future in situ screenings of potential metalloprotease inhibitors.

Labeling of Thermolysin in Yeast Cell Extract. To assess the feasibility of the affinity-based approach in potential large-scale proteomic experiments, we next labeled thermolysin in the presence of other proteins. In the recent report by Hagenstein et al., benzophenone was chosen as the photoactive label in their labeling experiments with kinases.[11] We therefore synthesized

(30) Fontana, A. *Biophys. Chem.* **1988**, *29*, 181−193.

(31) Leung, D.; Hardouin, C.; Boger, D. L.; Cravatt, B. F. *Nat. Biotechnol.* **2003**, *21*, 687−691.

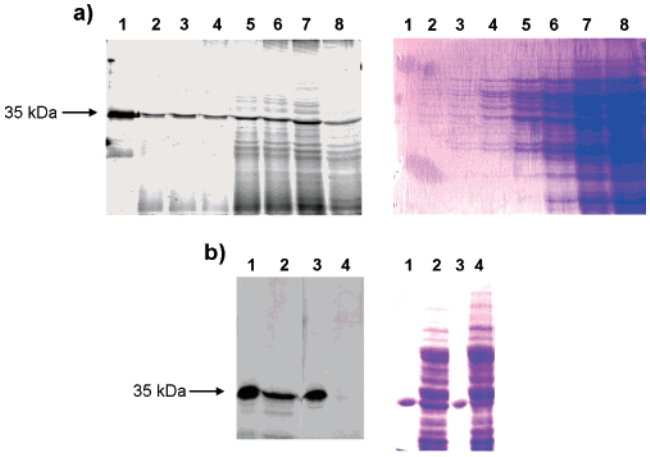

Figure 4. Affinity-based labeling of thermolysin spiked in crude yeast extracts. (a) Thermolysin (200 ng) was labeled with probe **5a** (5 μM) in the presence of increasing amounts of yeast total proteins: (lane 1) 0 μg (100%, e.g., pure thermolysin); (lane 2) 8 μg (2.5%); (lane 3) 20 μg (1%); (lane 4) 40 μg (0.5%); (lane 5) 80 μg (0.25%); (lane 6) 160 μg (0.13%); (lane 7) 320 μg (0.06%); (lane 8) 640 μg (0.03%) (percentage values in parentheses refer to relative amounts of thermolysin present in each reaction). Left panel: fluorescence image. Right panel: Coomassie stained gel. (b) Comparison of labeling specificity of diazirine- and benzophenone-based probes. **5a** and **6** (final concentration: 5 μM) were incubated with thermolysin (10 μg) alone or thermolysin + yeast extract (10 μg thermolysin + 100 μg total proteins): (lane 1) thermolysin + **5a**; (lane 2) thermolysin + yeast extract + **5a**; (lane 3) thermolysin + **6**; (lane 4) thermolysin + yeast extract + **6**. Left panel: fluorescence image. Right panel: Coomassie stained gel. Arrowed indicates the labeled thermolysin.

a benzophenone-containing GGL-NHOH probe, **6**, for the synchronous comparison with our diazirine-based probe, **5a**.[12]

Yeast extracts were prepared in which different amounts of total yeast proteins (0, 8, 20, 40, 80, 160, 320, and 640 μg, respectively) were spiked with 200 ng of thermolysin in a final reaction volume of 20 μL. The resulting extracts were labeled with **5a** (final concentration of the probe: 5 μM) and subsequently analyzed by SDS-PAGE followed by both fluorescence scanning and Coomassie staining (Figure 4a; left and right panels): **5a** was able to label the spiked thermolysin in the presence of differing amounts of yeast total proteins. As little as 0.03% of thermolysin in a large excess of the yeast extract (i.e., 200 ng in 640 μg total proteins) was successfully labeled (lane 8, left gel of Figure 4a). This detection limit for metalloproteases is comparable to that reported by Cravatt et al. in their version of activity-based MMP probes.[12] Also noticeable from the results were some background labelings in reactions where higher concentrations of yeast lysates were used (e.g. lanes 5−8), which may have arisen from the labeling of endogenous yeast metalloproteases present in the cell lysate (vide infra). Taken together, these experiments validate our affinity-based strategy to serve as an alternative approach to complement existing activity-based methods for potential large-scale protein profiling experiments.

To compare the difference between **5a** and **6** (the benzophenone-containing GGL-NHOH probe), 10 μg of thermolysin, both in pure form and spiked in the yeast extract (contains 100 μg of total proteins), were labeled with **5a** and **6** and subsequently analyzed by SDS-PAGE followed by both fluorescence scanning and Coomassie staining (Figure 4b, left and right gels): both probes were able to successfully label pure thermolysin (lanes 1 and 3, left gel in Figure 4b). However, the diazirine-based probe **5a** appeared to be a more superior labeling reagent than the benzophenone probe **6** in the spike experiment where a large excess of other proteins were present (lanes 2 and 4, left gel in Figure 4b). In fact, 5 μM benzophenone probe **6** failed to detect as much as 10% thermolysin spiked in the yeast cell lysate (e.g., 10 μg in 100 μg total proteins; lane 4, left gel in Figure 4b). On the other hand, 5 μM diazirine probe **5a** easily detected the same amount of thermolysin in the extract (lane 2, left gel in Figure 4b). With these results, together with earlier findings that **5a** was able to detect as little as 0.03% thermolysin in a crude yeast lysate (Figure 4a), we concluded that diazirine-based photoaffinity probes may provide better choices for potential proteomic profiling experiments by virtue of their high specificity and sensitivity in the detection of target proteins.

Large-Scale Profiling of Yeast Metalloproteases. All the labeling reactions presented thus far used commercial enzymes either in their purified forms or spiked into yeast cell lysates. To show the affinity-based labeling approach is equally amendable to large-scale proteomic experiments in which a large number of proteins are routinely involved, we next extended the approach to the large-scale study of a panel of yeast metalloproteases, cloned, expressed, and purified using standard large-scale protein expression protocols.[15] The open reading frames (ORF) of the 17 metalloproteases used in the study, together with the description of the gene products and their related literature references,[32−52] are listed in Table 2. The list encompasses many different yeast metalloproteases having a wide range of biological functions and subcellular distributions. Although the majority of the enzymes have the signature HEXXH motif which is common among yeast metalloproteases, they differ greatly in the substrates they act on. Hence, the nine probes, **5a**−**i**, differing only at their P_1 residues in the GG**X**-NHOH sequence, were used to individually label the metallo-

(32) Johnston, M. et al. *Science* **1994**, *265*, 2077−2082.
(33) Kull, F.; Ohlson, E.; Haeggström, J. Z. *J. Biol. Chem.* **1999**, *274*, 34683−34690.
(34) Lussier, M.; White, A. M.; Sheraton, J.; di Paolo, T.; Treadwell, J.; Southard, S. B.; Horenstein, C. I.; Chen-Weiner, J.; Ram, A. F.; Kapteyn, J. C.; Roemer, T. W.; Vo, D. H.; Bondoc, D. C.; Hall, J.; Zhong, W. W.; Sdicu, A. M.; Davies, J.; Klis, F. M.; Robbins, P. W.; Bussey, H. *Genetics* **1997**, *147*, 435−450.
(35) Zhang, N.; Ismail, T.; Wu, J.; Woodwark, K. C.; David Gardner, C. J.; Walmsley, R. M.; Oliver, S. G. *Yeast* **1999**, *15*, 1287−1296.
(36) Hunte, C.; Koepke, J.; Lange, C.; Rossmanith, T.; Michel, H. *Structure* **2000**, *8*, 669−684.
(37) Rawlings, N. D.; Barrett, A. J. *Biochem. J.* **1991**, *275*, 389−391.
(38) Tzagoloff, A.; Wu, M. A.; Crivellone, M. *J. Biol. Chem.* **1986**, *261*, 17163−17169.
(39) Oudshoorn, P.; Van Steeg, H.; Swinkels, B. W.; Schoppink, P.; Grivell, L. A. *Eur. J. Biochem.* **1987**, *163*, 97−103.
(40) Lopreiato, R.; Facchin, S.; Sartori, G.; Arrigoni, G.; Casonato, S.; Ruzzene, M.; Pinna, L. A.; Carignani, G. *Biochem. J.* **2004**, *377*, 395−405.
(41) Naitou, M.; Hagiwara, H.; Hanaoka, F.; Eki, T.; Murakami, Y. *Yeast* **1997**, *13*, 1275−1290.
(42) Tam, A.; Nouvet, F. J.; Kamada, F. K.; Slunt, H.; Sisodia, S. S.; Michaelis, S. *J. Cell Biol.* **1998**, *142*, 635−649.
(43) Schmidt, W. K.; Tam, A.; Michaelis, S. *J. Biol. Chem.* **2000**, *275*, 6227−6233.
(44) Trueblood, C. E.; Boyartchuk, V. L.; Picologlou, E. A.; Rozema, D.; Poulter, C. D.; Rine, J. *Mol. Cell. Biol.* **2000**, *20*, 4381−4392.
(45) Yang, M. J.; Geli, V.; Oppliger, W.; Suda, K.; James, P.; Schatz, G. *J. Biol. Chem.* **1991**, *266*, 6416−6423.
(46) Yang, M.; Jensen, R. E.; Yaffe, M. P.; Oppliger, W.; Schatz, G. *EMBO J.* **1988**, *7*, 3857−3862.
(47) Geli, V.; Yang, M. J.; Suda. K.; Lustig, A.; Schatz, G. *J. Biol. Chem.* **1990**, *265*, 19216−19222.
(48) Yao, T.; Cohen, R. E. *Nature* **2002**, *419*, 403−407.
(49) Verma, R.; Aravind, L.; Oania, R.; McDonald, W. H.; Yates, J. R.; Koonin, E. V.; Deshaies, R. J. *Science* **2002**, *298*, 611−615.
(50) Facchin, S.; Lopreiato, R.; Stocchetto, S.; Arrigoni, G.; Cesaro, L.; Marin, O.; Carignani, G.; Pinna, L. A. *Biochem. J.* **2002**, *364*, 457−463.
(51) Facchin, S.; Sarno, S.; Marin, O.; Lopreiato, R.; Sartori, G.; Pinna, L. A. *Biochem. Biophy. Res. Commun.* **2002**, *296*, 1366−71.
(52) Stocchetto, S.; Marin, O.; Carignani, G.; Pinna. L. A. *FEBS Lett.* **1997**, *414*, 171−175.

Table 2. List of 17 Yeast Metalloproteases Used in the Labeling Experiments with 5**a**[a]

ORF	gene name/synonym	description	reference
YHR113W		putative aspartyl aminopeptidase	32
YNL045W		similar to human leukotriene A_4 hydrolase	33
YHR132C		hypothetical protein in ACT3-YCK1 intergenic region, similarity to zinc carboxypeptidase; possible role in cell wall biogenesis and organization	34
YLL029W		probably an aminopeptidase for mitochondrial and nuclear processing; similar to *Rattus norvegicus* cytoplasmic aminopeptidase P and *Sus scrofa* aminopeptidase P	35
YIR027C	DAL1	allantoinase	
YPR191W	QCR2	core protein of ubiquinol cytochrome *c* reductase complex	36, 37, 38, 39
YBR281C		similarity to hypothetical protein YFR044C	
YKR038C	KAE1	hypothetical protein in DAL80-GAP1 intergenic region; similarity with O-sialoglycoprotease	40
YOL057W		probably a dipeptidyl peptidase	
YFR006W		hypothetical peptidase in the MPR1-GCN20 intergenic region; weak similarity to human X-Pro dipeptidase	41
YJR117W	STE24/AFC1	mediates the −COOH terminal CAAX proteolysis in a zinc-dependent manner and the first $-NH_2$ terminal cleavage during the biogenesis of yeast a-factor mating pheromone	42, 43, 44
YHR024C	MAS2	catalytic α-subunit of the mitochondrial processing peptidase (MPP)	45, 46, 47
YLR163C	MAS1	β-subunit of the mitochondrial processing peptidase (MPP)	45, 46, 47
YFR004W	RPN11/MPR1	subunit of the 26S proteasome lid subcomplex; strong similarity to *S. pombe* pad1 protein	48, 49
YGR262C	BUD32	serine/threonine protein kinase; important role in cell division and sporulation	40, 50, 51, 52
YPR024W	YME1	mitochondrial inner membrane protease of the AAA family; responsible for degradation of unfolded or misfolded mitochondrial gene products; role in mitochondrial organization and biogenesis	
YER078C		Peptidase of the PTP3-ILV1 intergenic region	

[a] Results were summarized in Figure 5.

proteases expressed as their glutatione-*S*-transferase (GST) fusions. Two nonmetalloprotease yeast proteins, also expressed as GST fusions, were used as control experiments.

All 19 yeast proteins were cloned, as Exclones, and expressed from their respectively yeast host cells following the vendor's protocols.[15] The resulting GST-fused proteins were purified to homogeneity on a glutathione (GSH)-containing affinity column. The expression and purification of each protein was unambiguously confirmed, as well as quantitated, by Coomasie staining and immunoblotting. Each protein was subsequently labeled with each of the nine probes. A negative control experiment with only GST was also run (data not shown). As shown in Figure 5, 12 out of the 17 different yeast metalloproteases tested were successfully labeled, albeit to different degrees by the nine probes used. No labeling was observed for GST, as well as the two negative controls (e.g., the nonmetalloprotease yeast proteins). The degree of labeling of each metalloprotease by the different probes was measured as a function of the relative fluorescence (RF) intensity internally calibrated to offset any difference in the relative protein expression level in each labeling reaction.

As shown in Figure 5, the difference in labeling with the nine probes is indicative of the diverse substrate specificities conferred by the 12 different yeast metalloproteases chosen. Each enzyme exerted a unique labeling profile which appears to correlate directly with its preference for different amino acids at the P_1 site of its potential substrate, indicating that our affinity-based approach could be extended to profile the substrate specificity of different metalloproteases in a gel-based proteomic experiment. This is exemplified in the labeling of four different

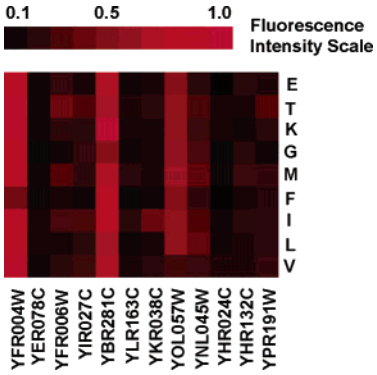

Figure 5. Plot of differential labeling profile of 12 yeast metalloproteases labeled with the 9 hydroxamate probes **5a**−**i** (final concentration: 5 μM). The yeast metalloproteases were labeled by their ORF names (*x* axis in the graph), and the probes used were identified by their one letter codes (*y* axis) according to the P_1 position.

yeast metalloproteases, namely YNL045W, YOL057W, YBR281C, and YFR004W. YNL045W codes for a bifunctional enzyme possessing an anion-activated leucinyl aminopeptidase activity and an epoxide hydrolase activity and exhibits 42% similarity to the human leukotriene A4 hydrolase. Using *p*-nitroanilide (*p*-NA) derivates of different amino acids, Kull et al. had previously shown that, under standard assay conditions,[33] the recombinant enzyme expressed from *E. coli* has the highest specific activity toward Leu-*p*-NA followed by Met-*p*-NA and Ala-*p*-NA, with Arg-, Glu-, and Gly-*p*-NA being poor substrates. This agrees well with our data where the RF signals observed for the Leu and Met probes were twice as high compared to the Glu probe (Figure 5). YOL057W codes for a probable

dipeptidyl aminopeptidase with no substrate specificity and exhibited a strong labeling with all the nine probes having different P_1 amino acids while YBR281C is similar to the glutamate carboxypeptidase-like protein encoded by the YFR044C ORF. An intriguing observation has been the labeling of YFR004W, which codes for a deubiquitinating (DUB) enzyme Rpn11/MPR1. Rpn11, a subunit of the yeast proteasome complex, comprises a highly conserved Jab1/MPN domain-associated metalloisopeptidase (JAMM) motif -$EX_nHXHX_{10}D$,[48] which is relatively unusual among common yeast metalloproteases. In our experiments, YFR004W was strongly labeled by most of the probes, possibly indicating that the affinity-based strategy is universal and therefore not restricted to only subclasses of metalloproteases having certain signature motifs.

For other yeast metalloproteases which were successfully labeled by our affinity-based probes, albeit with varying degrees, many of them are hitherto uncharacterized in the published literature, meaning that either their precise molecular functions are not known or they do not have defined substrate specificities. For instance, YER078C and YFR006W are similar to X-Pro aminopeptidases. YHR132C is similar to zinc-carboxypeptidase, while YKR078C is a putative glycoprotease. YIR027C is an allantoinase, while YPR024W is an essential mitochondrial inner member protease of the AAA family responsible for mitochondrial organization and biogenesis. YPR191W, a member of the petrilysin family of metalloendopeptidases, is a component of the ubiquinol cytochrome *c* reductase complex (complex III/ cytochrome bc_1 complex). It is required for the assembly of the complex. YHR024C/MAS2 codes for the α-subunit of the mitochondrial processing peptidase (MPP), which does not have any substrate specificity but recognizes some unique structural features, e.g., positively charged amphiphilic α-helices in a protein substrate, and there is some evidence to suggest that the border between the presequence and the mature protein is often marked by a β-sheet.[44] Geli et al. have shown that purified MAS2 exhibits little precursor cleavage activity by itself (less than 2% of the holo-protease) which probably explains the faint labeling seen with our probes.[46]

The common feature of all the above-described metalloproteases is that none of them has thus far been extensively studied in terms of their substrate specificities. Nevertheless, a unique fluorescence profile was obtained for each protein as a result of the affinity labeling approach. Our labeling strategy described herein may thus provide a novel and efficient approach for the characterization of these enzymes, as well as the identification of their potential substrates and candidate inhibitors.

Notably, five yeast metalloproteases tested in our experiments, YGR262C, YLR163C, YJR117W, YHR113W, and YLL029W, were not labeled by any of the nine probes. This could be due to one of the two reasons: (1) the protein is highly specific in its substrate requirement and thus failed to recognize and be subsequently labeled by any of the probes or (2) the expressed protein lacks catalytic activity, which may be caused by misfolding of the protein or other reasons. For example, YJR117W codes for membrane spanning CAAX protease (Afc1p) localized in the endoplasmic reticulum and involved in the processing of the N- and C-terminal portions of the yeast a-factor mating pheromone. The two cleavage sites are spatially separated and have little sequence similarity. Mutational studies with single amino acid substitutions have shown the protease is highly discriminating with single amino acid substitution at the cleavage site resulting in accumulation of the uncleaved product.[41,42] YLR163C/MAS1 is the β-subunit of the MPP and lacks any catalytic activity in the absence of its partner MAS2. Therefore it is not surprising that it was not labeled by any of our probes.

Conclusions

In conclusion, we have successfully developed an affinity-based, chemical proteomic approach which may be used for potential large-scale profiling of enzymes otherwise unattainable with current activity-based profiling approaches. By utilizing the noncovalent binding of easily accessible reversible inhibitors of an enzyme, the approach delivers a photoaffinity probe to the active site of the enzyme and subsequently modifies it covalently, rendering the resulting enzyme−probe complex detectable. We chose diazirine over benzophenone as the photolabile unit in our probes, as the diazirine-based probes were able to selectively label a small amount of the model metalloprotease from a crude yeast extract with high sensitivity and low background labeling. Using a repertoire of hydroxamate-based probes, we have also shown that the affinity-based approach described herein may be used not only for the large-scale identifications of metalloproteases but also for quick access to different labeling profiles of these enzymes, including their substrate "fingerprints" and inhibitory properties, etc.. Given the significant role many metalloproteases play in a variety of diseases, our approach may serve as a useful tool for potential therapeutics. The lack of covalent substrates for certain classes of enzymes limits the broad-range applicability of activity-based proteomic profiling as a diagnostic means of enzyme functionality. Our alternative strategy of affinity-based profiling thus provides a promising complementary approach to ABPP.

Acknowledgment. Funding support was provided by the National University of Singapore (NUS) and the Agency for Science, Technology and Research (A*STAR) of Singapore. S.Q.Y. is the recipient of the 2002 BMRC Young Investigator Award from the Biomedical Research Council of Singapore.

Supporting Information Available: Materials and methods, full details of dose-dependent inhibition experiments (including microplate- and gel-based experiments). This material is available free of charge via the Internet at http://pubs.acs.org.

JA047044I